Available online at www.sciencedirect.com
SCIENCE DIRECT®
Journal of Membrane Science 244 (2004) 55–68
journal of MEMBRANE SCIENCE
www.elsevier.com/locate/memsci

High pressure hydrogen permeance of porous stainless steel coated with a thin palladium film via electroless plating

Kurt S. Rothenberger[a,*], Anthony V. Cugini[a], Bret H. Howard[a], Richard P. Killmeyer[a], Michael V. Ciocco[b], Bryan D. Morreale[b], Robert M. Enick[c], Felipe Bustamante[c], Ivan P. Mardilovich[d], Yi H. Ma[d]

[a] *National Energy Technology Laboratory (NETL), US Department of Energy, P.O. Box 10940, Pittsburgh, PA 15236, USA*
[b] *NETL Support Contractor, Parsons, P.O. Box 618, South Park, PA 15129, USA*
[c] *NETL Research Associate, Chemical and Petroleum Engineering Department, University of Pittsburgh, Pittsburgh, PA 15261, USA*
[d] *Department of Chemical Engineering, Worcester Polytechnic Institute, Worcester, MA 01609, USA*

Received 2 July 2003; received in revised form 3 June 2004; accepted 15 June 2004
Available online 21 September 2004

Abstract

The high-pressure (100–2800 kPa) hydrogen permeance of two membranes, each composed of a thin palladium film (∼22 μm) deposited on the oxidized surface of a porous stainless steel tubular substrate (0.2 μm grade support) has been determined over the 623–723 K temperature range. The hydrogen flux was proportional to the H_2 partial pressure in the retentate raised to an exponent of ∼0.55 for one membrane and ∼0.64 for the other, indicating that the transport of hydrogen through the composite membrane was primarily limited by bulk diffusion. Overall, the hydrogen permeance of these membranes was within a wide range of values previously reported with thin film palladium membranes of comparable thickness. The first membrane exhibited no detectable helium flux at hydrogen partial pressures less than 350 kPa for a retentate stream composed of 90% hydrogen and 10% helium. H_2/He selectivity decreased to values as low as 12, however, at total transmembrane pressure differentials as great as 2800 kPa. As the membranes were heated from 623 to 723 K under pressures of up to 2800 kPa, the permeance of each membrane remained invariant at values of $\sim 1.5 \times 10^{-4}$ and $\sim 2.9 \times 10^{-4}$ mol/(m^2 s Pa$^{0.5}$), then decreased by ∼35% when the membrane was cooled back to 623 K, indicating some degradation of the membranes under the high-pressure testing conditions. Scanning electron microscopy (SEM) analysis revealed that extremes in the palladium film thickness ranged from about 10–50 μm with palladium "fingers" extending into the pore structure anchoring the palladium layer to the support. Although surface characterization could not pinpoint the source of the degradation, intermetallic diffusion could not be ruled out in spite of the presence of the oxide layer.

Keywords: Composite membranes; Gas separations; Membrane preparation and structure; Hydrogen; Permeability testing

1. Introduction

There are numerous possible industrial applications for palladium-based membrane reactors, including equilibrium-limited dehydrogenation reactions, reforming reactions and reactions that produce hydrogen as a product [1,2]. For example, hydrogen permeable membranes are an integral part of coal gasification plants being promoted by the US DOE Vision 21 program that employ the water-gas shift reaction to produce high purity hydrogen. In such cases, membrane reactors permit high conversions of carbon monoxide and steam to hydrogen and carbon dioxide to be attained via the selective removal of hydrogen from the effluent gas mixture. Palladium-based membranes continue to be considered as membrane candidates because of their catalytic activity with respect to hydrogen dissociation, high hydrogen permeability and resistance to oxidation. Some degree of success has been obtained in dealing with the potential drawbacks in the application of palladium membranes. Hydrogen embrittlement

* Corresponding author. Tel.: +1 412 386 6082; fax: +1 412 386 5920.
E-mail address: kurt.rothenberger@netl.doe.gov (K.S. Rothenberger).

0376-7388/$ – see front matter © 2004 Elsevier B.V. All rights reserved.
doi:10.1016/j.memsci.2004.06.036

of the membrane can be reduced through the use of highly permeable alloys such as 77 wt.% palladium–23 wt.% silver. The susceptibility of palladium surfaces to poisoning by trace concentrations of sulfur-containing gases in gasifier effluent streams (even after gas clean-up) is being diminished by the development of sulfur-resistant alloys such as the 60 wt.% palladium–40 wt.% copper alloy [3].

The expense of palladium is being mitigated by the development of technologies that deposit durable ultra-thin Pd layers on a porous substrate. There are numerous methods for manufacturing hydrogen membranes composed of thin films of palladium supported on porous substrates, including the use of thin palladium foils [1,4,5] or the deposition of palladium on a highly permeable, relatively low selectivity porous substrate [1,6–17]. In each case, the palladium film is designed to be thin enough to decrease material cost and increase hydrogen flux while remaining thick enough to retain adhesion, attrition resistance and mechanical integrity during temperature cycles. The porous substrate primarily provides mechanical integrity, though the substrate can also act as a low selectivity membrane. Although supported membranes require less palladium and exhibit higher permeance than bulk palladium, palladium delamination, cracks in the palladium layer, leaks at ceramic-metal seals, or pinhole defects can result in low selectivity. Further, the performance of palladium-coated porous stainless steel membranes may diminish at 700–900 K due to the formation of lower permeability alloys of palladium with substrate components [7,18]. Membrane failure at temperatures of approximately 673–773 K has also been reported for membranes consisting of thin palladium films supported on alumina, possibly due to sintering of the fine palladium grains [19] or irreversible changes in film structure due to annealing [20].

1.1. Membrane performance

The hydrogen flux through thin films of palladium is often directly proportional to the product of the hydrogen permeability, k, and the difference between the hydrogen partial pressures across the membrane raised to an exponent ($0.5 \leq n \leq 1$).

$$N_{H_2} = -k\frac{(P^n_{H_2,ret} - P^n_{H_2,perm})}{X_M} \quad (1)$$

The exponent is determined by optimizing the linear fit by varying the value of n in a plot of flux versus ($P^n_{H_2,ret} - P^n_{H_2,perm}$). Exponent values for thin supported membranes in the range of 0.5–1.0 have been reported for supported palladium, along with temperature-dependent exponents [14].

The hydrogen permeance, k', of a membrane is the ratio of the hydrogen permeability to the membrane thickness. Permeance is often calculated when the exact thickness of thin membranes is difficult to measure, or when the determination of the combined mass transfer resistances of the composite layers is desired.

$$k' = \frac{k}{X_M} \quad (2)$$

The permeance of bulk palladium membranes can therefore be determined from the slope of hydrogen flux plotted against ($P^n_{H_2,ret} - P^n_{H_2,perm}$).

Exponent values equal to 0.5 indicate that bulk diffusion limits the mass transport of hydrogen through the membrane. Greater exponent values ($0.5 < n < 1$) have been attributed to a variety of factors, including the increasing significance of surface effects, concentration dependence of the permeability (diffusion coefficient and/or solubility), gaseous flow through defects in thin palladium films, transport resistance of the substrate material, palladium surface contamination, flow of hydrogen through grain boundaries, thermal history, lattice dilatation and/or lattice defects. The direct proportionality of hydrogen flux to the pressure gradient across the membrane (i.e., $n = 1.0$) is indicative of the flux being surface-reaction controlled rather than bulk diffusion controlled [19,26].

1.2. Objective

Most prior studies of Pd-based hydrogen membranes have been conducted at relatively low temperatures and pressures. Membrane performance at the higher temperature and pressure conditions associated with the water-gas shift reactor proposed in conceptual coal-to-hydrogen gasification plants (473–1173 K, 1500–6800 kPa) has not been well documented.

Therefore, the primary objective of this study was to evaluate the performance of a thin, supported hydrogen membrane at temperatures as high as 723 K and hydrogen partial pressures as great as 2500 kPa. This performance was compared with literature reports of membranes evaluated at low hydrogen partial pressure conditions, particularly with a thin palladium membrane of comparable dimensions deposited on a porous ceramic substrate [30]. The membranes employed in this investigation were composed of a thin layer of palladium that was deposited on the oxidized surface of a porous stainless steel substrate via electroless plating. Membrane performance was characterized in terms of permeability, permeance, flux and selectivity.

A secondary objective of this study was to compare the performance of the membrane at high hydrogen partial pressure conditions with the numerous prior studies of thin supported palladium films characterized at low hydrogen partial pressure conditions. Although membrane permeance or permeability can be compared directly if the membranes are characterized by the same exponent value (e.g., $n = 0.5$), membranes with different hydrogen partial pressure exponent values should be compared by calculating the hydrogen flux at standard hydrogen partial pressures gradients on the retentate and sweep sides. Therefore, the hydrogen flux across each membrane was evaluated at “standard conditions” (a hydrogen pressure gradient of 100 kPa) as a means of comparing their performances.

2. Experimental section

2.1. Preparation of Pd membrane on porous stainless steel support

Porous 316L seamless stainless steel (SS) tubing, having an o.d. of 6.4 mm and an i.d. of 3.2 mm, was purchased from Mott Metallurgical Corporation. According to the manufacturer, the tube possesses a filter grade (95% exclusion) of 0.2 μm and a porosity of roughly 20–23%. The tube was cut into 45 mm long segments and welded to dense stainless steel tubes. The porous section of these units possessed approximately 9 cm^2 permeable surface area. The membrane was formed on the outer side of the porous tube by the electroless plating technique described elsewhere [7].

The applications of porous stainless steel supports are often limited at elevated temperatures due to the atomic diffusion of the components of the steel alloy into the palladium membrane which decreases the hydrogen permeability of the membrane. A simple and economical method for the formation of an intermediate layer on the porous stainless steel support to prevent the intermetallic diffusion was developed in the Worcester Polytechnic Institute (WPI) laboratory [37]. In this method, a thin metal oxide layer acting as a barrier to diffusion is formed on the surface of the support by controlled oxidation at high temperature using an oxidizing agent such as air or oxygen.

The metal oxide intermediate layer was prepared as follows. The porous stainless steel support was cleaned in an ultrasonic bath with alkaline solution at 333 K for 30 min. This cleaning procedure was followed by sequentially rinsing in tap water, deionized water and isopropanol. The alkaline cleaning solution consisted of a combination of alkaline sodium compounds such as hydroxide, carbonate, phosphate and organic detergent. After drying at 393 K for 2 h, the cleaned porous SS was oxidized with air at 673 K for about 10 h. The rate of heating and cooling during the oxidation process was 3 K/min.

The next step in membrane preparation was surface activation, the purpose of which was to seed the porous SS surface with palladium nuclei to initiate an autocatalytic process of the reduction of a metastable metal salt complex on the target surface during electroless plating. The activation procedure consisted of successive immersions in an acidic $SnCl_2$ solution (sensitizing) followed by an acidic $PdCl_2$ solution. After immersion in the $SnCl_2$ solution, a gentle rinsing with deionized water was used. Rinsing with 0.01 M HCl and then water was carried out after immersion in the $PdCl_2$ solution in order to prevent the hydrolysis of Pd^{2+} ions. The activation layer could be considered as a sandwich structure consisting of a number of thin layers, one after each sensitizing/activation cycle, with palladium nuclei on the top of each layer. A thicker activated layer resulted in a higher density of palladium nuclei on the support surface, but a diminished adhesion of further deposited palladium layers to the porous SS support. The optimum activated layer was created after three to six sensitizing/activation cycles.

The deposition of palladium on the outside surface of the activated porous SS supports was carried out at 333 K by placing the activated porous SS support in an electroless plating cell containing the plating solution. The plating cell was in turn immersed in a constant temperature bath. After about 90 min, the deposition rate of palladium decreased with the depletion of palladium ions and hydrazine, with a concomitant decrease in the pH of the plating solution. Because of this, the plating solution was replaced every 90 min with a fresh solution in order to maintain a stable, high-deposition rate. The membrane was carefully rinsed with deionized water after each plating cycle. The thickness of the palladium film was estimated gravimetrically; the increase in the mass of the porous stainless steel tube was assumed to be solely attributable to the deposition of the palladium film. The thickness was also measured by scanning electron microscopy (SEM) at NETL.

Three membranes were prepared for analysis. They were designated as NETL-Ma, in reference to the NETL facility where the membrane permeance and selectivity were determined and also in reference to Y.H. Ma of WPI, who supervised the membrane fabrication. One membrane was held out for destructive characterization prior to flux testing, and designated with the number “0.” The other two membranes were analyzed non-destructively before permeability testing, tested, then subjected to similar destructive post-test characterization. These were designated with the numbers “1” and “2.” The final number in the designation indicates the measured thickness of the palladium film (in microns).

2.2. Permeability testing

The membranes were tested both before and after shipment from WPI to NETL. The low pressure permeability testing unit at WPI has been described in detail elsewhere [7]. The unit consisted of a shell and tube assembly where the feed gas flowed upward through the shell side of the membrane and the permeate gas was collected on the tube side. The feed side was pressurized with the gas of interest (e.g., hydrogen), controlled with the help of a capacitance pressure transducer. The permeate side pressure was kept at atmospheric pressure. The gas permeation rate was determined by measuring the volumetric flow on the permeate side. Selectivity for hydrogen was verified by a lack of flow when nitrogen or helium was used as the feed gas.

The NETL hydrogen membrane testing (HMT) unit was designed and constructed for high-pressure, high-temperature membrane permeability testing. The apparatus was designed to allow simultaneous testing of hydrogen separation membranes at temperatures and pressures up to 1173 K and 2800 kPa, respectively. A schematic of the membrane apparatus is shown in Fig. 1 and has been described in detail elsewhere [38]. A supported palladium membrane was placed within 19.1 mm diameter Inconel 600® alloy tubing

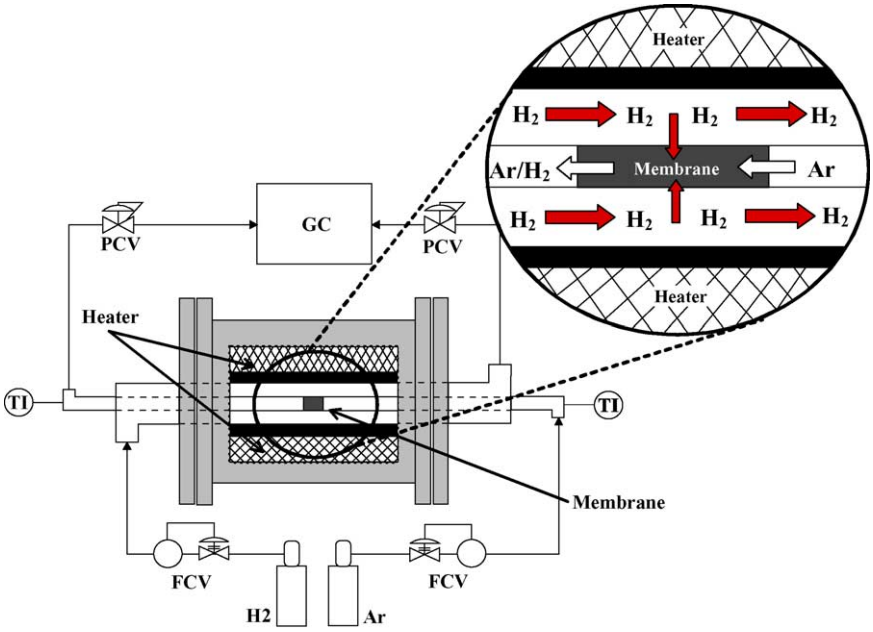

Fig. 1. High pressure, high temperature permeability apparatus and detail of the tubular membrane configuration.

which acted as the shell of the separation unit and allowed the membrane to be tested with counter current flow. The dimensions of the tested membranes are detailed in Table 1.

Membrane selectivity was determined using Eq. (3), where $\alpha_{H_2,He}$ is the selectivity for hydrogen over helium and $y_{gas,\ stream}$ is the mol% of either hydrogen or helium in the permeate or retentate stream, respectively. Helium served as the inert component in the feed stream (90 mol% H_2, 10 mol% He) to indicate the presence of leaks. A defect-free membrane exhibits an infinitely high selectivity value because helium cannot diffuse through palladium and its concentration in the permeate, $y_{He,\ permeate}$, would equal zero.

$$\alpha_{H_2,He} = \frac{y_{H_2,permeate}\, y_{He,retentate}}{y_{He,permeate}\, y_{H_2,retentate}} \quad (3)$$

The hydrogen–helium feed stream flow was controlled in the range of 200–1000 sccm. An argon sweep gas was passed axially over the permeate side of the membrane to minimize the accumulation of hydrogen at the membrane surface. However, in spite of these flow rates, the concentration of hydrogen in the sweep gas occasionally became quite high, sometimes exceeding 50 mol% hydrogen. The argon flow also was the means of transporting the diffusing hydrogen to the gas chromatograph for analysis. Mass flow controllers controlled the feed and sweep gas flow rates and pneumatically actuated stainless steel control valves regulated the pressure. Flows, pressures and temperatures were controlled with a personal computer-based process control system. The sweep gas pressure for the NETL-Ma-1-21.3 membrane test was maintained at atmospheric pressure, which generated pressure differentials as high as 2800 kPa, resulting in large mechanical strains across the membrane. By contrast, the sweep gas pressure during the NETL-Ma-2-22.2 membrane test was maintained approximately 138 kPa below the feed gas pressure in an effort to eliminate the effects of a large pressure drop across the thin palladium film.

Table 1
Dimensions of the membranes used for testing

	NETL-Ma-1-21.3	NETL-Ma-2-22.2
Membrane length (mm)	45	45
Membrane o.d. (mm)	6.35	6.35
Palladium thickness (mm)	21.3	22.2
Support average pore diameter (microns-μm)	0.2	0.2
Retentate shell i.d. (mm)	13.51	13.51

2.3. Membrane characterization

NETL-Ma-0-21.0 and NETL-Ma-1-21.3 were characterized by scanning electron microscopy and energy dispersive spectroscopy (EDS). The SEM was operated in backscattered-mode for elemental contrast. During destructive characterization, each membrane was cross-sectioned, and both its outer (palladium) surface and its cross-section were analyzed. The cross-section was obtained by cutting about half way through the membrane and breaking the remaining part. This method was used to avoid smearing the thin palladium layer and contaminating the support pores.

X-ray photoelectron spectroscopy (XPS) was used to examine the oxide passivation layer on the porous stainless steel support. NETL-Ma-0-21.0 and NETL-Ma-1-21.3 were characterized to determine surface components present as well as oxidation states.

3. Results and discussion

3.1. Permeance and permeability

Permeance and permeability results from this study have been summarized in Table 2, together with literature data from other thin-film palladium-based membranes, in such cases where the data could be extracted from the literature and presented on a common basis. The table is ordered according to membrane thickness. This unique collection of data allows for a uniform comparison of various types of thin-film palladium membranes from many different studies.

The flux of hydrogen through the NETL-Ma-0-21.0, NETL-Ma-1-21.3 and NETL-Ma-2-22.2 membranes was determined at WPI prior to shipment to NETL. Each membrane was tested for a minimum of 30 h at a temperature of 623 K, and pressure drops of up to 20 kPa. Separation factors were nearly ideal. Permeation data is given in Table 2. Permeance values, ranging from 3.3×10^{-4} to 4.2×10^{-4} mol/(m^2 s Pa$^{0.5}$) were within a factor of two of those recorded at NETL. Considering that the testing methods at the two locations were vastly different (low pressure with no permeate sweep versus large pressure range and swept permeate gas), this level of agreement is considered to be very good, and indicative that no changes to the membranes occurred upon shipment to NETL.

During testing at NETL, the flux of hydrogen through the NETL-Ma-1-21.3 membrane was determined sequentially at 623, 673, 723, and 623 K, while the flux through the NETL-Ma-2-22.2 membrane was evaluated at 623, 673, and 723 K. Flux values were plotted against ($P^n_{H_2,ret} - P^n_{H_2,perm}$), as represented in Eq. (1), to determine permeance and permeability. Two separate plots were made. In one plot, the exponent, n, was allowed to float to a "best fit" value. This value of 'n' is listed in Table 2. In the second method, done in order to promote comparison with other samples, the value of 'n' was forced to equal 0.5. Permeability and permeance values of each membrane at each temperature from these plots are provided in Table 2, along with the optimal exponent values for each run and the R^2 value associated with the best fit exponent or the fit to $n = 0.5$. The R^2 values associated with the fit of the data to a straight line ranged from 0.90 to 0.97 when n was set at 0.5 and from 0.94 to 0.99 when n was allowed to float, as shown in Table 2. These values were generally less than the values of 0.96–0.98 associated with NETL's study of unsupported bulk palladium [38].

An example permeability plot for the NETL-Ma-1-21.3 membrane at 623 K with $n = 0.5$ is shown in Fig. 2. The "S" shaped fit of the data around the straight line has been previously observed for flux data associated with a thin Pd–Cu alloy film supported on porous stainless steel [39]. It is believed to be an artifact of the data analysis, which does not adequately account for the fact that the concentration of hydrogen both decreases on the feed side and increases on the permeate side over the length of the tubular membrane along the direction of flow. This accounts for at least some of the poorer degree of fit than was observed in NETL's bulk Pd study, where relatively small disk membranes were employed [38].

The permeance of the NETL-Ma-1-21.3 and NETL-Ma-2-22.2 membranes employed in this study remained quite constant at values of $\sim 1.5 \times 10^{-4}$ and $\sim 2.9 \times 10^{-4}$ mol/(m^2 s Pa$^{0.5}$), respectively, over the 623–723 K temperature range when the exponent was constrained to a value of 0.5. Although permeability of bulk palladium [38] and palladium films deposited via electroless plating on ceramic substrates [30] is known to increase with temperature, the permeance of the NETL-Ma-1-21.3 and NETL-Ma-2-22.2 membranes remained invariant as they were heated from 623 to 723 K. Further, the NETL-Ma-1-21.3 membrane exhibited a 35% decrease in permeance, from 1.5×10^{-4} to 9.8×10^{-5} mol/(m^2 s Pa$^{0.5}$), when it was returned to its original temperature of 623 K. The invariance of the permeance (permeability) during heating and its subsequent loss upon cooling suggested that irreversible changes were taking place in the structure of the membrane that diminished the permeance of the thin palladium film. Such changes could have included physical deformation of the film or intermetallic diffusion between the palladium film and the porous stainless steel substrate. The latter possibility seems less likely, as the porous stainless steel was intended to be isolated from direct metal-metal contact with the active palladium layer by an oxide barrier layer. Such changes may have occurred throughout the test duration, with the diminished permeability from the structural changes masked by the increased permeability of bulk palladium with temperature; the net result being invariance in permeability in spite of increasing temperature.

The permeance of the palladium membranes of this study along with selected literature values is provided in Table 2 and shown in Fig. 3 for membranes characterized by a hydrogen partial pressure exponent of 0.5. In these calculations, any substrate materials are assumed to have infinite permeance, i.e., any resistance to flow is attributed to the palladium. The solid line corresponds to the NETL permeance correlation for 1000 μm thick bulk palladium membranes [38]. Both tested membranes exhibited permeance values that were about an order-of-magnitude greater than that of bulk palladium, as shown in Fig. 3. These permeance values were within the rather wide range of values for previously reported membranes of comparable thickness that were also characterized by a hydrogen partial pressure exponent of 0.5, as indicated by the results in Table 2 and Fig. 3.

As expected, Fig. 3 exhibits a great deal of scatter but there is a general trend of increasing permeance with decreasing membrane thickness. However, at some point there must be an upper limiting value of palladium permeance when the membrane permeance is no longer governed by bulk diffusion but instead becomes dominated by surface resistance effects. Upon examination of Fig. 3, this film thickness would appear to be less than 1 μm.

Bulk palladium exhibits very little difference in permeability for membrane thicknesses in the 100–10,000 μm

Table 2
NETL results (bold) with examples of literature data for permeability, permeance and flux of thin film palladium membranes

Reference	Year	Pd (μm)	T (K)	$1/T$ (1/K)	$P_{H_2,ret}$ (kPa)	$P_{H_2,per}$ (kPa)	n	R^2	k (mol/(m s Pa$^{0.5}$))	k' (mol/(m^2 s Pa$^{0.5}$))	N_{H_2} (mol/(m^2 s))
Wu et al. [21]	2000	0.35	673	0.00149	<101	<101	1		1.05E−12	3.00E−06	3.04E−01
Wu et al. [21]	2000	0.35	723	0.00138	<101	<101	1		1.40E−12	4.00E−06	4.05E−01
Wu et al. [21]	2000	0.35	773	0.00129	<101	<101	1		2.21E−12	6.30E−06	6.38E−01
Keuler et al. [22]	2002	1	603	0.00166	101–220	Sweep	1		1.10E−11	1.10E−05	1.11E+00
Keuler et al. [22]	2002	1	643	0.00156	101–220	Sweep	1		1.25E−11	1.25E−05	1.27E+00
Keuler et al. [22]	2002	1	683	0.00146	101–220	Sweep	1		1.30E−11	1.30E−05	1.32E+00
Keuler et al. [24]	2002	1	723	0.00138	101–220	Sweep	1		1.50E−11	1.50E−05	1.52E+00
Yeung et al. [23]	1999	1.6	623	0.00161	256	101	0.5		1.40E−10	8.80E−05	2.80E−02
Yeung et al. [23]	1999	1.6	850	0.00118	303	101	0.5		1.28E−09	8.00E−04	2.55E−01
Yan et al. [19]	1994	2	295	0.00339	100–200	Ar sweep	1		4.00E−15	2.00E−09	2.03E−04
Yan et al. [19]	1994	2	373	0.00268	100–200	Ar sweep	1		2.00E−13	1.00E−06	1.01E−01
Yan et al. [19]	1994	2	573	0.00175	100–200	Ar sweep	1		1.00E−11	5.00E−06	5.07E−01
Shu et al. [24]	1996	2	573	0.00175	105–120	N2 sweep	0.5		2.00E−09	1.00E−03	3.18E−01
Shu et al. [24]	1996	2	623	0.00161	105–120	N2 sweep	0.5		3.00E−09	1.50E−03	4.77E−01
Shu et al. [24]	1996	2	673	0.00149	105–120	N2 sweep	0.5		4.00E−09	2.00E−03	6.37E−01
Shu et al. [24]	1996	2	723	0.00138	105-120	N2 sweep	0.5		4.80E−09	2.40E−03	7.64E−01
Yan et al. [19]	1994	2	773	0.00129	100–200	Ar sweep	1		1.00E−11	5.00E−06	5.07E−01
Shu et al. [24]	1996	2	773	0.00129	105–120	N2 sweep	0.5		6.40E−09	3.20E−03	1.02E+00
Kusakabe et al. [17]	2001	3	573	0.00175	101.3	Ar sweep	1		7.50E−13	2.50E−07	2.53E−02
Kusakabe et al. [17]	2001	3	673	0.00149	101.3	Ar sweep	1		2.10E−12	7.00E−07	7.09E−02
Jun and Lee [15]	1999	3	723	0.00138	72	Vacuum	1		5.22E−11	1.74E−05	1.76E+00
Kusakabe et al. [17]	2001	3	773	0.00129	101.3	Ar sweep	1		6.00E−12	2.00E−06	2.03E−01
Kusakabe et al. [17]	2001	3	873	0.00115	101.3	Ar sweep	1		1.05E−11	3.50E−06	3.55E−01
Souleimanova et al. [25]	2002	4	673	0.00149	689	101	0.5		6.76E−10	1.69E−04	5.38E−02
Kusakabe et al. [26]	1996	4.4	673	0.00149	20–200	Ar sweep	1		4.40E−12	1.00E−06	1.01E−01
Kikuchi [27]	1995	4.5	666	0.00150	101	Sweep	0.5		4.02E−09	8.93E−04	2.84E−01
Kikuchi [27]	1995	4.5	769	0.00130	101	Sweep	0.5		6.03E−09	1.34E−03	4.27E−01
Jemaa et al. [28]	1996	6	673	0.00149	201	101	0.5		2.26E−09	3.76E−04	1.20E−01
Souleimanova et al. [25]	2002	8	673	0.00149	689	101	0.5		1.31E−09	1.64E−04	5.22E−02
Li et al. [29]	2000	10	740	0.00135	203	101	0.65		2.80E−09	2.80E−04	5.02E−01
Collins and Way [30]	1993	11.4	823	0.00122	156–2445	101–140	0.6		3.23E−09	2.83E−04	2.85E−01
Collins and Way [30]	1993	11.4	873	0.00115	156–2445	101–140	0.57		5.84E−09	5.13E−04	3.66E−01
Uemiya et al. [31]	1991c	13	673	0.00149	196	101	0.5		1.68E−08	1.19E−03	3.79E−01
Uemiya et al. [31]	1991c	13	773	0.00129	196	101	0.5		2.05E−08	1.46E−03	4.65E−01
Collins and Way [30]	1993	17	723	0.00138	156–2445	101–140	0.62		2.34E−09	1.38E−04	1.75E−01
Collins and Way [30]	1993	17	773	0.00129	156–2445	101–140	0.59		4.04E−09	2.38E−04	2.14E−01
Collins and Way [30]	1993	17	823	0.00122	156–2445	101–140	0.56		6.82E−09	4.01E−04	2.55E−01
Collins and Way [30]	1993	17	873	0.00115	156–2445	101–140	0.55		9.96E−09	5.86E−04	3.32E−01
Ma-0-19.7 (WPI)	2003	19.7	623	0.00161	101–202	101	0.5		8.29E−09	4.21E−04	1.34E−01
DeRossett [5]	1960	20	616	0.00162	108–4925	101–2169	0.8		9.24E−11	4.62E−06	4.67E−02
Kikuchi [27]	1995	20	666	0.00150	101	Sweep	0.5		4.66E−09	2.33E−04	7.42E−02
DeRossett [5]	1960	20	672	0.00149	108–4925	101–2169	0.8		1.18E−10	5.90E−06	5.96E−02
Uemiya et al. [32]	1991a	20	673	0.00149	150–394	101	0.76		2.33E−10	1.16E−05	7.39E−02
Uemiya et al. [33]	1991b	20	675	0.00148	297	101	0.5		7.21E−09	3.61E−04	1.15E−01
Uemiya et al. [33]	1991b	20	725	0.00138	297	101	0.5		8.52E−09	4.26E−04	1.36E−01
DeRossett [5]	1960	20	727	0.00138	108–4925	101–2169	0.8		1.26E−10	6.30E−06	6.37E−02
Kikuchi [27]	1995	20	769	0.00130	101	Sweep	0.5		6.54E−09	3.27E−04	1.04E−01
Shu et al. [34]	1994	20	773	0.00129	136	He sweep	0.5		8.93E−09	4.47E−04	1.42E−01
Uemiya et al. [33]	1991b	20	775	0.00129	297	101	0.5		9.17E−09	4.59E−04	1.46E−01
Collins and Way [30]	1993	20	823	0.00122	156–2445	101–140	0.53		1.43E−08	7.15E−04	3.22E−01
Paturzo and Basile [35]	2002	21	753	0.00133	160–201	101	1		2.60E−09	5.46E−14	5.53E−09
Ma-1-21.3 (WPI)	2003	21.3	623	0.00161	101–202	101	0.5		7.22E−09	3.39E−04	1.08E−01
NETL-Ma-1-21.3	**2003**	**21.3**	**623**	**0.00161**	**95–2573**	**Sweep (<67)**	**0.5**	**0.97**	**3.25E−09**	**1.53E−04**	**4.85E−02**
NETL-Ma-1-21.3	**2003**	**21.3**	**673**	**0.00149**	**95–2573**	**Sweep (<67)**	**0.5**	**0.97**	**3.22E−09**	**1.51E−04**	**4.81E−02**
NETL-Ma-1-21.3	**2003**	**21.3**	**723**	**0.00138**	**95–2573**	**Sweep (<67)**	**0.5**	**0.97**	**3.04E−09**	**1.43E−04**	**4.54E−02**
NETL-Ma-1-21.3	**2003**	**21.3**	**623**	**0.00161**	**95–2573**	**Sweep (<67)**	**0.5**	**0.93**	**2.09E−09**	**9.80E−05**	**3.12E−02**
NETL-Ma-1-21.3	**2003**	**21.3**	**623**	**0.00161**	**95–2573**	**Sweep (<67)**	**0.62**	**0.98**	**5.47E−10**	**2.57E−05**	**3.37E−02**
NETL-Ma-1-21.3	**2003**	**21.3**	**673**	**0.00149**	**95–2573**	**Sweep (<67)**	**0.61**	**0.98**	**6.34E−10**	**2.98E−05**	**3.45E−02**
NETL-Ma-1-21.3	**2003**	**21.3**	**723**	**0.00138**	**95–2573**	**Sweep (<67)**	**0.62**	**0.98**	**5.34E−10**	**2.51E−05**	**3.22E−02**

Table 2 (*Continued*)

Reference	Year	Pd (μm)	T (K)	$1/T$ (1/K)	$P_{H_2,ret}$ (kPa)	$P_{H_2,per}$ (kPa)	n	R^2	k (mol/(m s Pa$^{0.5}$))	k' (mol/(m^2 s Pa$^{0.5}$))	N_{H_2} (mol/(m^2 s))
NETL-Ma-1-21.3	**2003**	**21.3**	**623**	**0.00161**	**95–2573**	**Sweep (<67)**	**0.72**	**0.99**	**9.56E−11**	**4.49E−06**	**1.78E−02**
Lin et al. [18]	1998	22	623	0.00161	202–1515	101	0.5		2.57E−09	1.17E−04	3.72E−02
Lin et al. [18]	1998	22	623	0.00161	202–1515	101	0.5		6.01E−09	2.73E−04	8.69E−02
Ma-2-22.2 (WPI)	2003	22.2	623	0.00161	101–202	101	0.5		7.45E−09	3.35E−04	1.07E−01
NETL-Ma-2-22.2	**2003**	**22.2**	**623**	**0.00149**	**95–2573**	**Sweep (<300)**	**0.5**	**0.93**	**7.15E−09**	**3.22E−04**	**1.02E−01**
NETL-Ma-2-22.2	**2003**	**22.2**	**673**	**0.00149**	**95–2573**	**Sweep (<300)**	**0.5**	**0.90**	**5.97E−09**	**2.69E−04**	**8.55E−02**
NETL-Ma-2-22.2	**2003**	**22.2**	**723**	**0.00138**	**95–2573**	**Sweep (<300)**	**0.5**	**0.92**	**5.95E−09**	**2.68E−04**	**8.53E−02**
NETL-Ma-2-22.2	**2003**	**22.2**	**623**	**0.00161**	**95–2573**	**Sweep (<300)**	**0.53**	**0.94**	**4.69E−09**	**2.11E−04**	**9.28E−02**
NETL-Ma-2-22.2	**2003**	**22.2**	**673**	**0.00161**	**95–2573**	**Sweep (<300)**	**0.53**	**0.91**	**3.98E−09**	**1.79E−04**	**7.96E−02**
NETL-Ma-2-22.2	**2003**	**22.2**	**723**	**0.00149**	**95–2573**	**Sweep (<300)**	**0.58**	**0.97**	**1.89E−09**	**8.52E−05**	**6.59E−02**
Mardilovich et al. [7]	1998	24	623	0.00161	151–404	<101.3	0.5		7.41E−09	3.09E−04	9.84E−02
Mardilovich et al. [7]	1998	24	623	0.00161	151–404	<101.3	0.5		3.67E−09	1.53E−04	4.87E−02
Mardilovich et al. [7]	1998	24	673	0.00149	151–404	<101.3	0.5		6.70E−09	2.79E−04	8.88E−02
Mardilovich et al. [7]	1998	24	723	0.00138	151–404	<101.3	0.5		8.69E−09	3.61E−04	1.15E−01
Tosti et al. [4]	2000	50	593	0.00169	200	Sweep	0.5		9.64E−09	1.93E−04	6.14E−02
Tosti et al. [4]	2000	50	623	0.00161	200	Sweep	0.5		1.08E−08	2.16E−04	6.88E−02
Jarosch and de Lasa [36]	2001	156	1023	0.00098	425–603	Sweep	0.5		4.14E−09	2.65E−05	8.44E−03
Jarosch and de Lasa [36]	2001	156	1123	0.00089	425–603	Sweep	0.5		5.24E−09	3.36E−05	1.07E−02
Jarosch and de Lasa [36]	2001	244	523	0.00191	425–603	Sweep	0.5		4.23E−09	1.74E−05	5.54E−03
Jarosch and de Lasa [36]	2001	244	823	0.00122	425–603	Sweep	0.5		1.58E−08	6.47E−05	2.06E−02

Notes: N_{H_2} flux calculations based on permeance at reported T, $P_{H_2,retentate}$ = 101.3 kPa, $P_{H_2,sweep}$ = 0 kPa.

range [38]. Interestingly enough, the apparent permeability of thin, supported Pd membranes (0.1–100 μm) is actually *less* than that of bulk palladium. This is most readily observed by comparing the permeability values in Table 2 that correspond to n = 0.5, as illustrated in Fig. 4. Our recent correlation for the permeability of bulk palladium over a wide range of temperature and pressure is provided to facilitate the comparison of thin film palladium permeability with the permeability of bulk palladium [38]. Although the literature data is widely scattered, there is a general trend of decreasing permeability with decreasing membrane thickness below 100 μm. Another way of stating this is that the permeability, a quantity intended to be independent of membrane thickness, is actually not independent once thickness becomes less than about 100 μm. This has been attributed to many causes including the increased influence of surface effects, concentration dependence of the permeability, transport resistance of the substrate material, palladium surface contamination,

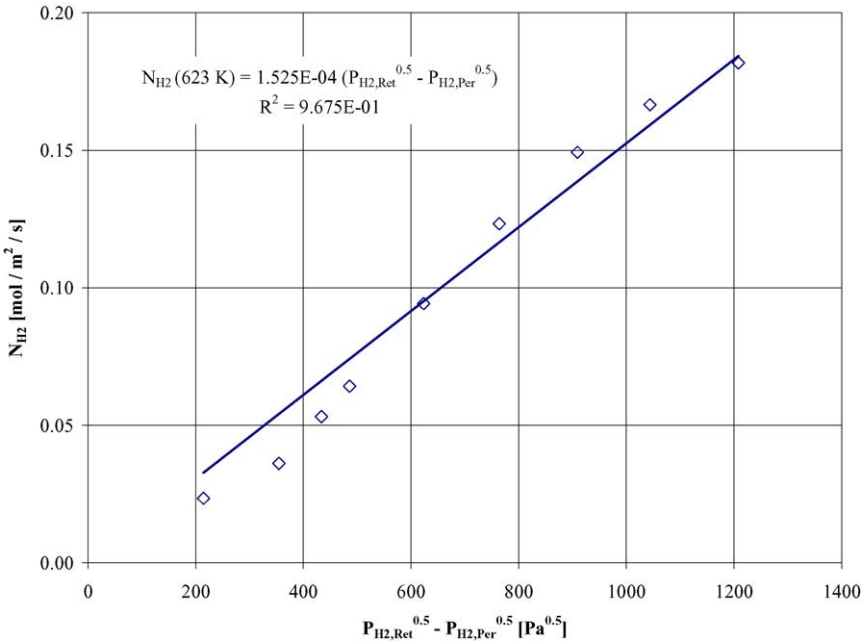

Fig. 2. Flux of hydrogen through the membranes as a function of the difference between the square root of the hydrogen partial pressures on the retentate and sweep side of the membrane. The line represents the best fit of data for the NETL-Ma-1-21.3 membrane the first time it was maintained at 623 K.

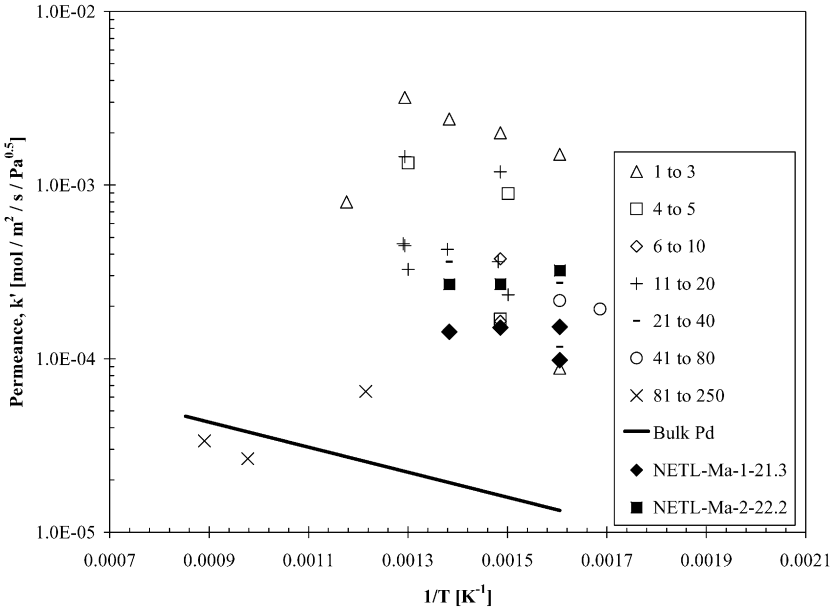

Fig. 3. Permeance of palladium as a function of membrane thickness (in μm) and temperature; $n = 0.5$; data and references listed in Table 2. The solid line corresponds to 1 mm thick bulk palladium [38]. The sequence of the NETL-Ma-1-21.3 membrane (♦) was $1000\,T^{-1} = 1.61, 1.49, 1.38, 1.62$; the sequence of the NETL-Ma-2-22.2 membrane (■) was $1000\,T^{-1} = 1.61, 1.49, 1.38$.

flow of hydrogen through grain boundaries, thermal history, lattice dilatation and/or lattice defects.

Although the permeability of thin supported palladium membranes decreased with decreasing thickness shown in Fig. 4, the permeance values increased, as was shown in Fig. 3. However, the increase was not as great as would have been expected by the purely inverse relationship between permeance and thickness given in Eq. (2). This again demonstrates the increasing importance of surface resistance, rather than diffusion, on hydrogen transport, as membrane thickness decreases.

3.2. Flux comparisons based on reference conditions

Although permeance and permeability relationships are valuable in characterizing the general behavior of a mem-

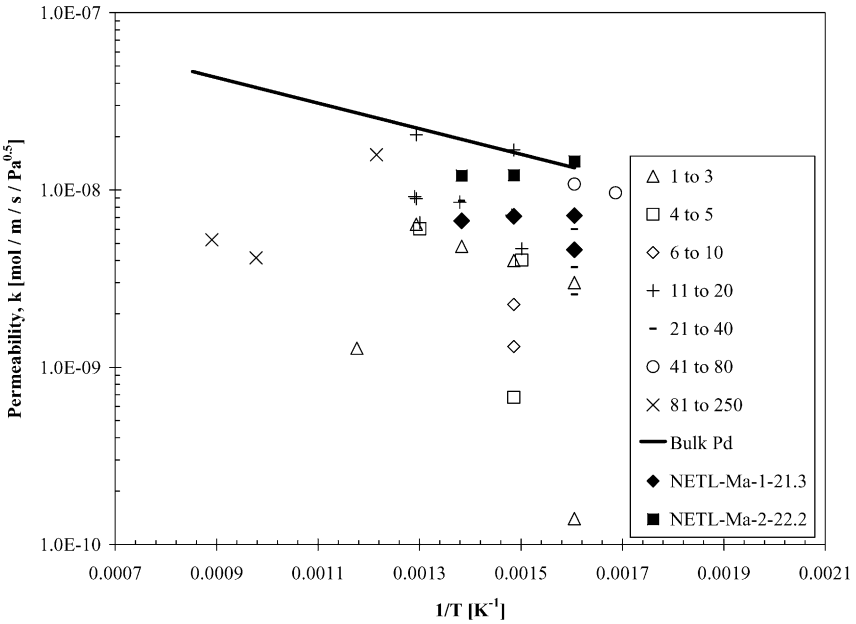

Fig. 4. Permeability of palladium as a function of membrane thickness (in μm) and temperature; $n = 0.5$; data and references listed in Table 2. The solid line corresponds to 1 mm thick bulk palladium [38]. The sequence of the NETL-Ma-1-21.3 membrane (♦) was $1000\,T^{-1} = 1.61, 1.49, 1.38, 1.62$; the sequence of the NETL-Ma-2-22.2 membrane (■) was $1000\,T^{-1} = 1.61, 1.49, 1.38$.

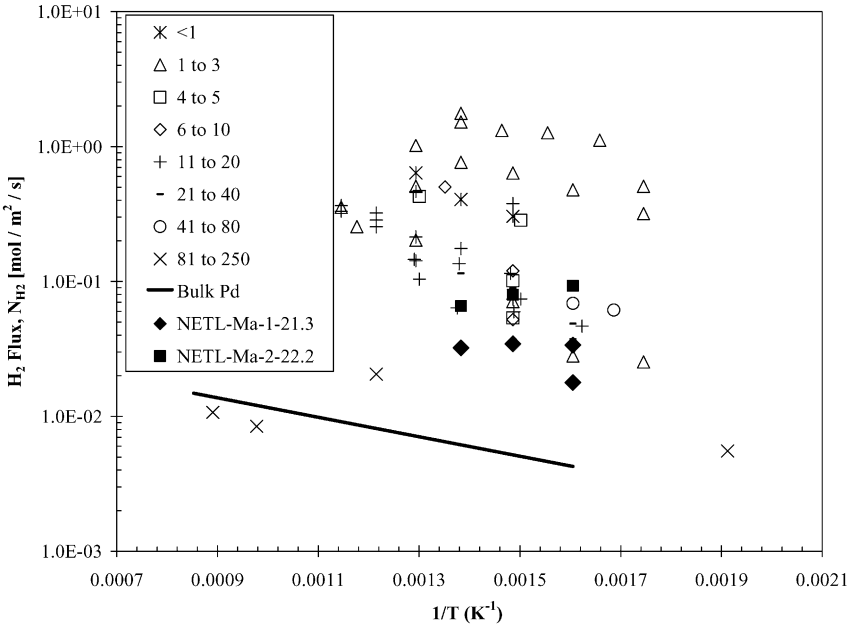

Fig. 5. Flux of hydrogen through palladium as a function of membrane thickness (in μm) and temperature for hydrogen partial pressure of 101.3 kPa on the retentate side and 0 on the permeate side; $0 < n < 1$; data and references listed in Table 2. The solid line corresponds to 1 mm thick bulk palladium [38]. The sequence of the NETL-Ma-1-21.3 membrane (♦) was 1000 T^{-1} = 1.61, 1.49, 1.38, 1.62; the sequence of the NETL-Ma-2-22.2 membrane (■) was 1000 T^{-1} = 1.61, 1.49, 1.38.

brane material, a more practical question is how a given membrane might perform in a specific situation. To illustrate this for the tested and literature thin-film palladium membranes, a reference condition was arbitrarily chosen so that all the membranes, characterized by partial pressure exponents ranging from 0.5 to 1.0, could be compared. The expected flux was based on a retentate hydrogen partial pressure of 100 kPa and a permeate hydrogen partial pressure of zero at the actual temperature at which the membrane was evaluated. The membrane permeance and partial pressure exponent values listed in Table 2 were used to estimate the flux at the reference pressure condition using Eq. (1). These flux calculation results are listed in the last column of Table 2 and are illustrated in Fig. 5. The results, though useful, must be viewed with a degree of caution. The permeability and permeance relationships are a very broad measure of material behavior. They are particularly sensitive to the choice of the best fit exponent, *n*. For example, the flux of the NETL-Ma-1-21.3 membrane at 673 K was 4.8×10^{-2} mol/m^2 s when calculated using the permeability relationship with $n = 0.5$, but 3.5×10^{-2} mol/m^2 s when calculated using the best fit exponent of $n = 0.61$ (Table 2). These two values, differing by almost 40%, were calculated from the *same set* of experimental data, with the only difference being how the original data was fit.

As expected, Fig. 5 shows the general trend of increasing flux with decreasing palladium thickness. The flux of submicron palladium layers was comparable to the flux of 1 μm thick palladium, indicative of the enhanced influence of surface effects, rather than bulk diffusion, on hydrogen flux for these ultra-thin membranes.

The NETL-Ma membranes exhibited flux values roughly an order-of-magnitude greater than bulk palladium and were consistent with fluxes calculated for previously reported membranes of comparable thickness. In particular, the membrane studied by Collins and Way [30] was prepared by electroless deposition, was comparable in thickness, and was characterized over similar ranges of temperature and pressure as the NETL-Ma membranes. The porous substrates differed, however, as the palladium membranes investigated by Collins and Way were supported on porous ceramic while the NETL-Ma palladium membranes were supported on porous stainless steel. At 723 K, fluxes associated with the 17 μm thick palladium membrane of Collins and Way averaged 1.75×10^{-1} mol/m^2 s, roughly two to four times greater than the fluxes of 3.2×10^{-2} mol/m^2 s for the NETL-Ma-1-21.1 and 6.6×10^{-2}mol/m^2 s NETL-Ma-2-22.2 micron palladium films. When differences in testing methods, membrane thickness, and the previously cited imprecision in calculating fluxes from permeance/permeability relationships are taken into account, this agreement is quite reasonable. It should also be noted that the flux of the NETL-Ma membranes had likely already begun to degrade at 673 K as previously discussed.

3.3. Membrane selectivity

The NETL-Ma-1-21.3 membrane exhibited infinite selectivity, α, at total pressure drops less than 350 kPa (at the detection limit of the gas chromatograph). However, at higher pressure differentials across the membrane, helium was detected on the permeate side, as illustrated in Fig. 6.

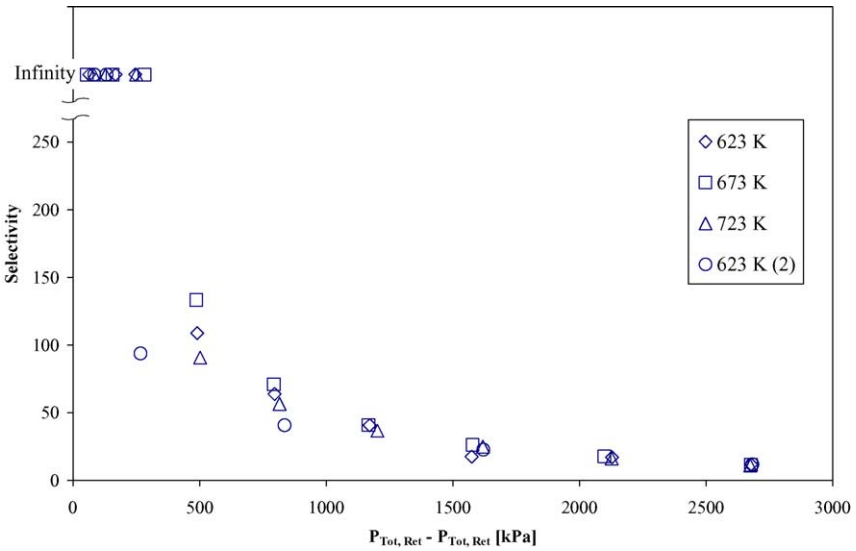

Fig. 6. Selectivity of NETL-Ma-1-21.3 as a function of total pressure drop across the membrane.

The selectivity decreased from a value of 135 at a total pressure drop of 500 kPa to a value of 12 as the total pressure drop increased to 2800 kPa. No hysteresis in selectivity was observed as the total pressure drop was decreased. These results indicate that high selectivity of a thin palladium film composite membrane at low total pressure drop conditions does not ensure that high selectivity will be realized at elevated pressure drop conditions. The NETL-Ma-2-22.2 membrane, which was not subject to a pressure differential greater than 138 kPa because the permeate sweep gas was maintained at approximately the same pressure as the retentate stream, exhibited infinite selectivity at all conditions.

3.4. Characterization of the membranes

NETL-Ma-0-21 was examined by SEM in an as-prepared condition to provide a baseline for comparison to a membrane after flux testing to determine whether any observable morphological changes had occurred. The external surface of this membrane consisted of a bimodal coverage of rounded hillocks ranging from about 5 to 25 μm in diameter (Fig. 7a). Some areas of the membrane surface consisted of densely packed hillocks of high relief (Fig. 7a, upper left corner) while other areas were of much lower relief (Fig. 7a, rest of image). These features probably resulted from a combination of preferential palladium deposition on some surface sites during the electroless plating process as well as a reflection of the underlying topology of the substrate material. Also evident are a few surface pits that are generally less than 10 μm in diameter.

SEM analysis of the fracture cross-section of the as-prepared membrane revealed several interesting morphological characteristics of the palladium coating (Fig. 7b and c). The average palladium layer thickness appeared to be about 20–25 μm, in good agreement with the thickness estimated using the gravimetric method. Extremes in palladium film thickness ranged from about 10 to about 50 μm, however, as shown in Fig. 7b. Resulting from the method of palladium application, palladium “fingers” were seen to extend into the pore structure. This probably acted as a mechanical anchor holding the palladium layer to the support. Closer examination of the fractured edge of the palladium layer (Fig. 7c) showed that the layer appeared to contain internal voids. Also evident was some smaller-scale layering within the palladium layer (Fig. 7c). Sub-micron palladium islands (bright spots) were visible on the pore walls immediately below the palladium membrane layer (Fig. 7d). These islands probably resulted from early-stage palladium deposition on surface activated sites. Sealing of the surface of the porous substrate which blocked palladium-solution access probably prevented continued growth of these islands.

NETL-Ma-1-21.3 was examined by SEM after flux testing. The appearance of this membrane was very similar to the fresh membrane, with no obvious changes attributed to flux testing. The external surface of this membrane consisted of a uniform coverage of rounded hillocks ranging from about 10 to 100 μm in diameter (Fig. 8a). Again, these features probably resulted from a combination of preferential palladium deposition on some surface sites during the electroless plating process as well as a reflection of the underlying topology of the substrate material. Some surface pits, generally less than 10 μm in diameter, were evident in this membrane.

SEM analysis of the fracture cross-section of the used membrane revealed similar morphological characteristics as observed in the fresh membrane (Fig. 8b and c). As observed for the fresh membrane, the average palladium layer thickness appeared to be about 20–25 μm. Extremes in palladium film

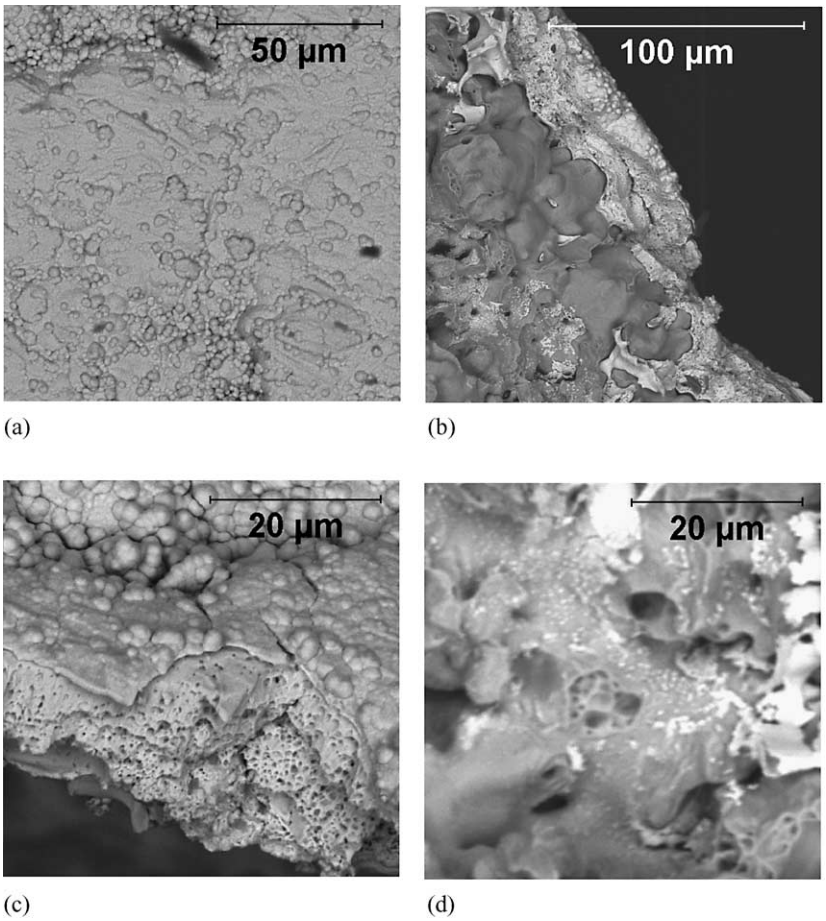

Fig. 7. SEM images of a palladium membrane before flux testing. (a) Typical SEM image of membrane surface showing rounded hillocks. Cross-section of membrane surface showing (b) palladium "fingers;" (c) layering and internal voids; and (d) sub-micron palladium islands (bright spots) on pore walls immediately below the palladium membrane layer.

thickness ranged from about 10 to about 50 μm, as shown in Fig. 8b and c. Palladium "fingers" again extended into the pore structure. Closer examination of the fractured edge of the palladium layer (Fig. 8d) showed that the layer appeared to contain internal voids. The fractured edge also suggested that the "fingers" extending into the pores of the substrate are hollow. Sub-micron palladium islands were also visible on the pore walls immediately below the palladium membrane layer (Fig. 8d).

Intermetallic diffusion occurring between the porous support and the active membrane layer resulting in the formation of a lower permeability alloy has been proposed to explain the observed flux decrease following testing at 723 K. For this diffusion to occur, the oxide passivation layer would have had to allow migration of metal atoms between the porous support and the active membrane layer. A possible mechanism that would allow this migration to occur would be the reduction of the oxide layer. The conditions under which the membranes were tested are conducive to metal oxide reduction, i.e., elevated temperature under flowing hydrogen which would also carry the byproduct water away. However, chromium oxide is not easily reduced under such mild conditions so it would be expected to persist as a diffusion barrier. EDS was used to investigate the composition of the palladium membrane layer to determine if any detectable levels of substrate component metals (primarily Fe, Cr, and Ni) had migrated into the palladium layer. Not surprisingly, the results were inconclusive. The sensitivity limits and the sample morphology made obtaining a dependable analysis difficult. Analysis of the oxide coating on the supporting porous stainless steel was attempted by XPS. A comparison of the fresh versus the post-test membrane was done to determine if any reduction of the surface oxide occurred. These analyses were also inconclusive. However, for one sample of used support, evidence of the reduction of iron in the oxide layer to metallic iron was observed. In the Fe 2p region for this sample, a small peak was observed at a binding energy lower than the binding energy typical for oxidized iron. This peak suggests that at least some of the iron in the oxide layer was reduced. No similar peaks were observed for Cr or Ni. Thus, the possibility of intermetallic diffusion can neither be supported nor ruled out from these observations.

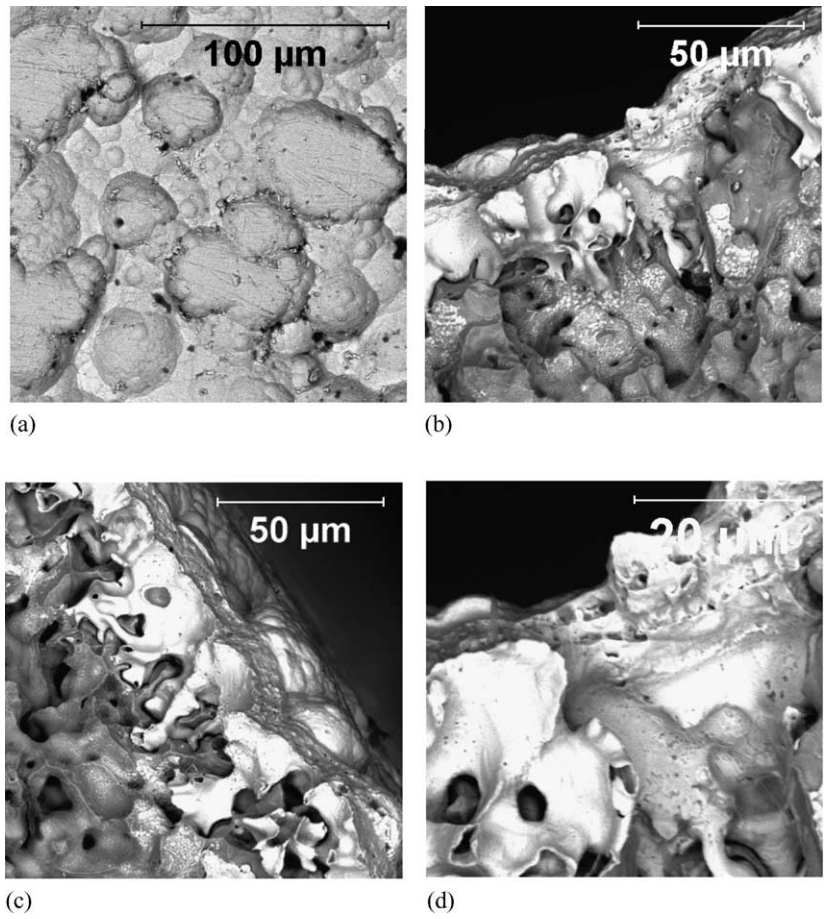

Fig. 8. SEM images of a palladium membrane after flux testing. (a) Typical SEM image of membrane surface after testing. Pits are visible as black spots. Cross-section of membrane surface showing (b) palladium fingers; (c) thickness variation; and (d) internal voids.

4. Conclusions

Membranes composed of thin films of palladium (21–22 μm) deposited on porous stainless steel via electroless plating have been evaluated at temperatures of 623–723 K, total pressure drops to 2800 kPa, and hydrogen partial pressures up to 2500 kPa. Although the membranes exhibited infinite selectivity for hydrogen in the absence of a total pressure drop or in the presence of a small pressure drop across the membrane, H_2/He selectivity decreased from infinity at pressure drops below 350 kPa to 12 at 2800 kPa. This decrease in selectivity was attributed to viscous flow of the retentate through the defects and illustrated that excellent membrane selectivity at low total pressure drop conditions does not ensure infinite selectivity at elevated pressure drop conditions. The optimal exponent values for the partial pressure of hydrogen in the flux expression were 0.55 and 0.64 for the two membranes, indicating that hydrogen transport was limited by bulk diffusion rather than surface effects. The membranes exhibited permeance and permeability values that were within the rather wide range of literature values reported for supported membranes of comparable thickness. The severity of the test conditions may have contributed to the degradation of the membrane, which exhibited a drop of 35% in permeance at 623 K after cycling to 723 K at pressure drops of up to 2800 kPa. Although the exact source of the degradation could not be pinpointed, intermetallic diffusion could not be ruled out, despite the presence of a thin barrier oxide layer. Characterization also revealed a fairly rich and complex morphology of the palladium film, including the presence of palladium "fingers" that extended into and appeared to anchor the palladium layer to pore structure, smaller scale layering within the overall palladium layer, and internal voids in the palladium structure.

Acknowledgement and disclaimer

The Hydrogen Membrane Testing unit at NETL was operated and maintained by the Engineering Technicians of Parsons Federal Services, Inc.—Ronald Hirsh, Paul Dieter, Ronald Benko, Jeremy Brannen, Michael Ditillo, Stephen Lopez, Brian Neel, and Raymond Rokicki. Reference in this paper to any specific commercial product, process, or service is to facilitate understanding and does not imply its endorsement or favoring by the US Department of Energy.

Nomenclature

$\alpha_{H_2,He}$	selectivity for hydrogen over helium
k	hydrogen permeability of metal (mol/(m s $Pa^{0.5}$))
k'	hydrogen permeance of metal (mol/(m^2 s $Pa^{0.5}$))
n	pressure exponent, 0.5–1.0
N_{H_2}	flux of hydrogen molecules (mol H_2/(m^2 s))
P	total pressure (Pa)
P_{H_2}	hydrogen molecule partial pressure (Pa)
$P_{H_2,perm}$	hydrogen molecule partial pressure on permeate side (Pa)
$P_{H_2,ret}$	hydrogen molecule partial pressure on retentate side (Pa)
R^2	Pearson product moment correlation coefficient
T	temperature (K)
X_M	membrane thickness (m)
$y_{H_2,permeate}$	concentration of hydrogen in the permeate stream (mol%)
$y_{H_2,retentate}$	concentration of hydrogen in the retentate stream (mol%)
$y_{He,permeate}$	concentration of helium in the permeate stream (mol%)
$y_{He,retentate}$	concentration of helium in the retentate stream (mol%)

References

[1] J. Shu, B. Grandjean, A. Van Neste, S. Kaliaguine, Catalytic palladium-based membrane reactors: a review, Can. J. Chem. Eng. 69 (1991) 1036.

[2] S. Uemiya, State-of-the-art of supported metal membranes for gas separation, Sep. Purif. Methods 28 (1999) 51.

[3] D.J. Edlund, A catalytic membrane reactor for facilitating the water-gas-shift reaction at high temperatures, Phase II, Final Report to the US DOE on Grant DE-FG03-91ER81229 Bend Research, 1995.

[4] S. Tosti, L. Bettinali, V. Violante, Rolled thin Pd and Pd–Ag membranes for hydrogen separation and recovery, Int. J. Hydrogen Energy 25 (2000) 319.

[5] A. DeRossett, Processing gases at high pressures, diffusion of hydrogen through palladium membranes, Ind. Eng. Chem. 52 (1960) 525–528.

[6] S. Goto, S. Assabumrungrat, T. Tagawa, P. Praserthdam, The effect of direction of hydrogen permeation on the rate through a composite palladium membrane, J. Membr. Sci. 175 (2000) 19.

[7] P.P. Mardilovich, Y. She, Y.H. Ma, M.H. Rei, Defect-free palladium membranes on porous stainless-steel support, AIChE J. 44 (1998) 310.

[8] K. Yeung, A. Varma, Novel preparation techniques for thin metal-ceramic composite membranes, AIChE J. (1995) 2131.

[9] K. Yeung, J. Sebastian, A. Varma, Novel preparation of Pd/Vycor composite membranes, Catal. Today 25 (1995) 231.

[10] R.S. Souleimanova, A.S. Mukasyan, A. Varma, Study of structure formation during electroless plating of thin metal-composite membranes, Chem. Eng. Sci. 54 (1999) 3369.

[11] A. Basile, A. Criscuoli, F. Santella, E. Drioli, Membrane reactor for water gas shift reaction, Gas Sep. Purif. 10 (1996) 243–254.

[12] L. Huang, C. Chen, Z. He, D. Peng, G. Meng, Palladium membranes supported on porous ceramics prepared by chemical vapor deposition, Thin Solid Films (1997) 98.

[13] S. Nam, S. Lee, K.H. Lee, Preparation of a palladium alloy composite membrane supported in a porous stainless steel by vacuum electrodeposition, J. Membr. Sci. 153 (1999) 163.

[14] H.B. Zhao, K. Pflanz, J.H. Gu, A.W. Li, N. Stroh, H. Brunner, G.X. Xiong, Preparation of palladium composite membranes by modified electroless plating procedure, J. Membr. Sci. 142 (1998) 147.

[15] C.S. Jun, K.H. Lee, Preparation of palladium membranes from the reaction of $Pd(C_3H_3)(C_5H_5)$ with H_2: wet-impregnated deposition, J. Membr. Sci. 157 (1999) 107.

[16] N. Fernandes, S. Fisher, J. Poshusta, D. Vlachos, M. Tsapatsis, J. Watkins, Reactive deposition of metal thin films within porous supports from supercritical fluids, Chem. Mater. 13 (2001) 2023.

[17] K. Kusakabe, M. Takahashi, H. Maeda, S. Morooka, Preparation of thin palladium membranes by a novel method based of photolithography and electrolysis, J. Chem. Eng. Jpn. 34 (2001) 703.

[18] Y.M. Lin, G.L. Lee, M.H. Rei, An integrated purification and production of hydrogen with a palladium membrane-catalytic reactor, Catal. Today 44 (1998) 343.

[19] S. Yan, H. Maeda, K. Kusakabe, S. Morooka, Thin palladium membrane formed in support pores by metal-organic chemical vapor deposition method and application to hydrogen separation, Ind. Eng. Chem. Res. 33 (1994) 616.

[20] S.N. Paglieri, K.Y. Foo, J.D. Way, J.P. Collins, D.L. Harper-Nixon, A new preparation technique for Pd/alumina membranes with enhanced high-temperature stability, Ind. Eng. Chem. Res. 38 (1999) 1925.

[21] L.Q. Wu, N. Xu, J. Shi, Preparation of a palladium composite membrane by an improved electroless plating technique, Ind. Eng. Chem. Res. 39 (2000) 342.

[22] J. Keuler, L. Lorenzen, S. Miachon, Preparing and testing Pd films of thickness 1–2 micrometer with high selectivity and high hydrogen permeance, Sep. Sci. Technol. 37 (2002) 379.

[23] K. Yeung, S. Christiansen, A. Varma, Palladium composite membranes by electroless plating technique, relationship between plating kinetics, film microstructure and membrane performance, J. Membr. Sci. 159 (1999) 107.

[24] J. Shu, B. Grandjean, A. Van Neste, S. Kaliaguine, A. Giroir-Fendler, J. Dalmon, Hysteresis in hydrogen permeation through palladium membranes, J. Chem. Soc. Faraday Trans. (1996) 2475.

[25] R.S. Souleimanova, A.S. Mukastan, A. Varma, Dense Pd-composite membranes prepared by electroless plating and osmosis: synthesis, characterization and hydrogen permeation studies, AIChE J. 48 (2002) 262.

[26] K. Kusakabe, S. Yokoyama, S. Morooka, J. Hayashi, H. Nagata, Development of supported thin palladium membrane and application to enhancement of propane aromatization on Ga-silicate catalyst, Chem. Eng. Sci. 51 (1996) 3027.

[27] E. Kikuchi, Palladium/ceramic membranes for selective hydrogen permeation and their application to membrane reactor, Catal. Today 25 (1995) 333.

[28] N. Jemaa, J. Shu, S. Kaliaguine, B. Grandjean, Thin palladium film formation on shot peening modified porous stainless steel substrates, Ind. Eng. Chem. Res. 35 (1996) 973.

[29] A. Li, W. Liang, R. Hughes, Fabrication of dense palladium composite membranes for hydrogen separation, Catal. Today 56 (2000) 45.

[30] J.P. Collins, J.D. Way, Preparation and characterization of a composite palladium-ceramic membrane, Ind. Eng. Chem. Res. 32 (1993) 3006.

[31] S. Uemiya, N. Sato, H. Ando, T. Matsuda, E. Kikuchi, Separation of hydrogen through palladium thin films supported on a porous glass tube, J. Membr. Sci. 56 (1991) 303.
[32] S. Uemiya, N. Sato, H. Ando, E. Kikuchi, The water-gas shift reaction assisted by a palladium membrane reactor, Ind. Eng. Chem. Res. 67 (1991) 585.
[33] S. Uemiya, N. Sato, H. Ando, T. Matsuda, E. Kikuchi, Steam reforming of methane in a hydrogen-permeable membrane reactor, Appl. Catal. 667 (1991) 223.
[34] J. Shu, B. Grandjean, S. Kaliaguine, Methane steam reforming in asymmetric Pd- and Pd–Ag/porous SS membrane reactors, Appl. Catal. A 119 (1994) 305.
[35] L. Paturzo, A. Basile, Methane conversion to syngas in a composite palladium membrane reactor with increasing number of Pd layers, Ind. Eng. Chem. Res. 41 (2002) 1703.
[36] K. Jarosch, H. de Lasa, Permeability and selectivity, and testing of hydrogen diffusion membranes suitable for use in steam reforming, Ind. Eng. Chem. Res. 40 (2001) 5391.
[37] Y.H. Ma, P.P. Mardilovich, Y. She, Hydrogen gas-extraction module and method of fabrication, US Patent 6,152,987 (2000).
[38] B.D. Morreale, M.V. Ciocco, R.M. Enick, B.I. Morsi, B.H. Howard, A.V. Cugini, K.S. Rothenberger, The permeability of hydrogen in bulk palladium at elevated temperatures and pressures, J. Membr. Sci. 212 (2003) 87.
[39] Y.H. Ma, I.P. Mardilovich, E.E. Engwall, Thin composite palladium and palladium/alloy membranes for hydrogen separations., in: N.N. Li, E. Drioli, W.W. Ho, G.G. Lipscomb (Eds.), Advanced Membrane Technology. Annu. N. Y. Acad. Sci., 984, 2003, pp. 346–360.